Structure and properties of two polymorphs of tetra-n-butylammonium bis(maleonitriledithiolato)platinate(1-)

Mochida, Tomoyuki

Nagabuchi, Eri

Ueda, Mikio

(Citation)
Inorganica Chimica Acta,363(14):4108-4111

(Issue Date)
2010-11-25

(Resource Type)
journal article

(Version)
Accepted Manuscript

(URL)
https://hdl.handle.net/20.500.14094/90001802

Note

Structure and properties of two polymorphs of tetra-*n*-butylammonium bis(maleonitriledithiolato)platinate(1−)

Tomoyuki Mochida[a,b,*], Eri Nagabuchi[a], and Mikio Ueda[a†]

[a]*Department of Chemistry, Faculty of Science, Toho University, Miyama, Funabashi, Chiba 274-8510, Japan*

[b]*Department of Chemistry, Graduate School of Science, Kobe University, Rokkodai, Nada, Hyogo 657-8501, Japan*

Abstract

Structural determination of tetra-*n*-butylammonium bis(maleonitriledithiolato)platinate(1−), a polymorphic compound, revealed that one polymorph consists of a columnar arrangement of dimers of the anion and is isomorphous with a corresponding nickelate complex. In contrast to the nickelate complex, the complex exhibited no spin-Peierls transition; strong antiferromagnetic interactions were observed between the anions due to dimerization in the column. The other polymorph consists of a tetramer unit of the anion.

Keywords: Crystal structure; Platinum complex; Polymorphism; Magnetic property

---

*Corresponding Author. Tel/fax: +81-78-803-5679

E-mail address: tmochida@platinum.kobe-u.ac.jp (T. Mochida)

†Present address: Wayo Konodai Girls' High School, Ichikawa, Chiba.

1. Introduction

Metal dithiolene complexes are versatile π-conjugated molecules that are frequently employed as components of molecular conductors and magnets [1]. Among these, $[M(mnt)_2]$ (mnt = maleonitriledithiolato) anions often form one-dimensional columnar molecular arrangements, and have drawn attention due to their low-dimensional electronic properties. In particular, spin-Peierls-like paramagnetic-diamagnetic phase transitions [2] and ferromagnetic interactions [3,4,5] in $[Ni(mnt)_2]$ salts have attracted special interest. Our studies on ferrocenium salts of $[M(mnt)_2]$ revealed supramolecular structures and phase transition phenomena [6]. Examples of $[Pt(mnt)_2]$ salts are fewer, but they also exhibit phase transitions [7] and their electronic properties are of interest.

In previous work, we performed structural characterization of $(NBu_4)[Ni(mnt)_2]$ and $(NBu_4)_2[Co(mnt)_2]_2$ [8,9]. Because the nickel complex exhibits a first-order paramagnetic-diamagnetic phase transition at around 170 K [10], we were interested in the results when different metal atoms were used. We report herein the crystal structures and magnetic properties of two polymorphs of $(NBu_4)[Pt(mnt)_2]$ (Fig. 1). One of the polymorphs (α-form) was found to be isomorphous with the corresponding nickel salt, and exhibited strong antiferromagnetic interactions. In contrast to the nickelate complex, the complex exhibited no spin-Peierls transition due to stronger dimerization. The structure of the other polymorph (β-form) was found to be isomorphous with that already determined by Kirmse (CCDC 57234) [11].

2. Results and Discussion

2.1. Crystal structures

The complex exhibited polymorphism, forming block crystals (α-form) and plate crystals (β-form). Figure 2(a) shows the packing diagram of the α-form, which was found to be isomorphous with $(NBu_4)[Ni(mnt)_2]$. The space group of the crystal is *C*2/c. The cell volume

of the complex, V = 6080.6(6) Å^3, is greater than that of the isomorphous nickel salt (V = 6014(3) Å^3), reflecting the larger ionic radius of platinum. The crystal contains one crystallographically independent anion. The intramolecular Pt···S bond lengths are virtually identical to those of other $[Pt(mnt)_2]^-$ salts [12]. The anions form dimers and are stacked in columnar fashion along the *c*-axis. The arrangement of anions is shown in Fig. 2(b), together with the intermolecular distances. Within the dimer, the molecular long axes of the anions are parallel, and the anions are in a slipped configuration such that the central metal atom of one anion is positioned above one of the S atoms in the other anion, with a Pt···S distance of 3.813(1) Å. The dimers are canted with respect to each other, interacting *via* a Pt···S contact of 3.738(1) Å, and the intradimer and interdimer Pt···Pt distances are 3.8680(3) and 4.6574(3) Å. In the isomorphic nickel salt $(NBu_4)[Ni(mnt)_2]$, the corresponding intradimer and interdimer Ni···Ni distances are 3.9963(8) and 4.5263(8) Å. Thus, the degree of dimerization is stronger in the platinum salt. In addition, in the nickel complex, the intradimer and interdimer Ni···S distances are the same (3.715 Å) at room temperature [8]. The anion columns are surrounded by tetrabutylammonium cations, in which the butyl groups adopt an all-*trans* conformation. The thermal ellipsoid of one of the terminal methyl groups, C(16), is elongated, which indicates a slight disorder.

In the crystal structures of $(NEt_4)[M(mnt)_2]$ (M = Pt, Ni), the anions also form columnar arrangements with dimerization [13,14], but there is interdimer contact between the sulfur atoms and the structures are different from those of the complexes under discussion.

To obtain a qualitative evaluation of the intermolecular interactions, intermolecular overlap integrals between the SOMO orbitals were calculated based on the extended Hückel molecular orbital method. In the platinum complex, the overlap integrals within the dimer (*S1*) and between the dimer (*S2*) are 9.24×10^{-3} and 4.92×10^{-3}, respectively. Thus, the intradimer interaction is twice the strength of the interdimer interaction. For intermolecular

configurations of [M(mnt)$_2$] with Pt···S-type interactions, ferromagnetic interactions may appear when the intermolecular overlap integral is small [3,4], but the values for the complexes under discussion are large. Calculations for the room temperature structure of the nickel complex [8] afforded overlap integrals within the dimer (*S1*) and between the dimer (*S2*) of 3.72×10^{-3} and 5.41×10^{-3}, respectively. These data support the stronger tendency toward dimerization in the platinum complex.

The packing diagram of the β-form, viewed along the *a*-axis, is shown in Fig. 3(a). As the structure has already been determined [11], we will give only a brief description of the structure in order to discuss intermolecular interactions, based on our redetermination data. The structure is isomorphic with the corresponding Au salt [15]. The space group is *P*–1 and there are two crystallographically independent [Pt(mnt)$_2$] anions in the crystal. The crystal consists of tetramer units of the anions, as shown in Fig. 3(b). Two molecules form a centrosymmetric dimer (anions I and I'), and the other two (anions II and II') are located on both sides of the dimer. Within the central dimer, the intermolecular S···S distance was found to be 3.760(2) Å, and between anions I and II, the Pt···S distances were found to be 3.935(2) and 3.958(2) Å. There is no significant intermolecular interaction between the tetramers.

Intermolecular overlap integrals for the SOMO orbitals were also calculated for this complex. The overlap integrals between molecules I and I' (*S1*) and molecules I and II (*S2*) are 11.6×10^{-3} and 2.55×10^{-3}, respectively; *S1* was four times the value of *S2*. This shows that strong interaction exists within the central dimer, as the value is comparable to that of the dimer unit in the α-form. The overlap integral between tetramers is 1.00×10^{-3}, which is far smaller than those within the tetramer.

2.3. Magnetic susceptibilities

The magnetic susceptibilities for the α-form are shown in Fig. 4 in the form of χT versus

T plots. The χT value was ca. 0.22 emu K mol^{-1} at room temperature, which is much smaller than the value expected for non-interacting $S = 1/2$ spins (= 0.375 emu K mol^{-1}). The value decreased with decreasing temperature, and the complex became almost diamagnetic below 70 K. This indicates the presence of strong intermolecular antiferromagnetic interactions.

The acceptor columns can be regarded as alternating antiferromagnetic chains with $S = 1/2$, with J_1 and J_2 interactions operating in alternating fashion. The magnetic exchange energy (J) is proportional to the square of the transfer integral (t), $J \sim 4t^2/U_{\mathrm{eff}}$, where U_{eff} is the on-site Coulomb repulsive energy, and $t = -ES$ (eV), where $E = 10$ eV [16]. Using these relationships and based on the results of overlap integral calculations, J_1/J_2 was estimated to be 1:0.28. Although the magnetic data may be better analyzed using the Ising model [4,17], the data were analyzed based on the alternating Heisenberg chain model ($J < 0$), taking into account the rather small anisotropy in the g-values and the high temperature range of fitting. The theoretical molar susceptibility is given by the following equation [18]:

$$\chi = \frac{Ng^2\mu_B^2}{k_BT}\frac{A + Bx + Cx^2}{1 + Dx + Ex^2 + Fx^3},$$

where $x = |J|/k_BT$ ($J < 0$), and A–F are a set of parameters that are dependent on J_2/J_1 (= α). The expression is derived from the spin Hamiltonian $H = -2J \Sigma [S_{2i} \cdot S_{2i-1} + \alpha S_{2i} \cdot S_{2i+1}]$. In the analysis, $g = 2.034$ [19] and $\alpha = 0.28$ were used for fitting the data. The best-fit parameters were $J_1/k_B = -230$ K and $J_2/k_B = -64$ K. The fitting deviates somewhat from the experimental data, but the parameters obtained, which indicate strong antiferromagnetic interactions, are reasonable considering the crystal structure. The magnetic structure of the β-form can be viewed as an antiferromagnetic four-spin system, taking into consideration the result of the overlap integral calculations. Magnetic characterization was not performed for this compound due to its small yield.

3. Experimental

The complex $(NBu_4)[Pt(mnt)_2]$ was prepared according to the literature method [20]. Black block crystals of the α-form were obtained by vapor diffusion of pentane into an ethyl acetate solution of the compound. Crystals obtained from ethyl acetate were mostly α-form but sometimes contained a small amount of the β-form, which were black plate crystals and could be isolated under a microscope. The β-form crystals were also obtained by vapor diffusion of diethyl ether into a dichloromethane solution of the compound. These polymorphs could not be distinguished by infrared spectroscopy. The temperature dependence of magnetic susceptibility was obtained from 300 to 2 K using a Quantum Design MPMS-XL SQUID magnetometer under a magnetic field of 5000 G. The core diamagnetic components were corrected by calculation from Pascal's constants. The intermolecular overlap integrals between the SOMO orbitals were calculated based on the extended Hückel molecular orbital method, using a software package developed by Prof. T. Mori (Tokyo Institute of Technology) [21].

X-ray diffraction data for single crystals were collected at room temperature on a Bruker SMART APEX CCD diffractometer equipped with a graphite crystal and incident beam monochromator using Mo Kα radiation (λ = 0.71073 Å). The frames were integrated by using the Siemens SAINT+ program [22], and the data were corrected for absorption by using the SADABS program [23]. The structures were solved by the direct method (SHELXS 97 [24]) and expanded using Fourier techniques. The non-hydrogen atoms were refined anisotropically. The hydrogen atoms were placed at idealized positions and allowed to ride on the relevant heavier atoms. Crystallographic parameters of the α-form are listed in Table 1. Crystallographic data (excluding structure factors) for the structures in this paper have been deposited with the Cambridge Crystallographic Data Centre as supplementary publication nos. CCDC 255520 (α-form) and 255521 (β-form). These data can be obtained free of charge from

the Cambridge Crystallographic Data Centre via www.ccdc.cam.ac.uk/data_request/cif.

Acknowledgment

We thank Y. Funasako (Kobe University) for data analysis. This work was supported financially by a Grant-in-Aid for Scientific Research in Priority Areas (No. 16038224, Novel functions of molecular conductors under extreme conditions) and the "High-Tech Research Center" Project 2005–2009 from MEXT (Ministry of Education, Culture, Sports, Science and Technology of Japan). We also thank Mr. Masaru Nakama (WarpStream Tokyo, Co., Ltd.) for providing Web-based database systems.

References

[1] (a) C. Faulmann, P. Cassoux, Prog. Inorg. Chem. 52 (2003) 399, and references cited therein; (b) C. L. Beswick, J. M. Schulman, E. I. Stiefel, Prog. Inorg. Chem. 52 (2003) 55, and references cited therein; (c) S. Alvarez, R. Vicente, R. Hoffmann, J. Am. Chem. Soc. 107 (1985) 6253.

[2] (a) X. Ren, Y. Chen, C. He, S. Gao, J. Chem. Soc., Dalton Trans. (2002) 3915; (b) J. Xie, X. Ren, C. He, Y. Song, Q. Meng, R. K. Kremer, Y. Yao, Chem. Phys. Lett. 369 (2003) 41.

[3] (a) A.T. Coomber, D. Beljonne, R. H. Friend, J. L. Brédas, A. Charlton, N. Robertson, A. E. Underhill, M. Kurmoo, P. Day, Nature 380 (1996) 144; (c) M. Uruichi, K. Yakushi, Y. Yamashita, J. Qin, J. Mat. Chem. 8 (1998) 141.

[4] J. Nishijo, E. Ogura, J. Yamaura, A. Miyazaki, T. Enoki, T. Takano, Y. Kuwatani, M. Iyoda, Solid State Commun. 116 (2000) 661.

[5] B. L. Ramakrishna, Inorg. Chim. Acta 114 (1986) 31.

[6] (a) T. Mochida, T. Koinuma, T. Akasaka, M. Sato, Y. Nishio, K. Kajita, H. Mori, Chem. Eur. J. 13 (2007) 1872-1881; (b) T. Mochida, K. Takazawa, H. Matsui, M. Takahashi, M.

Takeda, M. Sato, Y. Nishio, K. Kajita, H. Mori, Inorg. Chem. 44 (2005) 8628; (c) T. Mochida, H. Matsui, S. Suzuki, H. Moriyama, Mol. Cryst. Liq. Cryst. 376 (2002) 295.

[7] (a) A. E. Pullen, C. Faulmann, I. I. Pokhodnya, P. Cassoux, M. Tokumoto, Inorg. Chem. 37 (1998) 6714. (b) M. Matos, G. Bonfait, R. T. Henriques, M. Almeida, Phys. Rev. B, 54 (1996) 15307. (c) X. M. Ren, H. Okudera, R. K. Kremer, Y. Song, C. He, Q. J. Meng, P. H. Wu, Inorg. Chem. 43 (2004) 2596. (d) J. Xie, X. Ren, Y. Song, W. Tong, C. Lu, Y. Yao, Q. Meng, Inorg. Chem. Commun. 5 (2002) 395.

[8] T. Mochida, S. Suzuki, H. Moriyama, H. Terao, T. Sugawara, Acta Cryst. C56 (2000) 1183.

[9] T. Mochida, K. Takazawa, M. M. Matsushita, T. Sugawara, Acta Cryst. C58 (2002) m431.

[10] R. D. Willett, C. J. Gomez-Garcia, B. L. Ramakrishna, B. Twamley, Polyhedron, 24 (2005) 2232.

[11] R. Kirmse, S. Saluschke, CSD refcode: ZINLAJ; CCDC 57234, unpublished results (1996).

[12] D. Bellamy, A. Christofides, N. G. Connelly, G. R. Lewis, A. G. Orpen, P. Thornton, J. Chem. Soc., Dalton Trans. (2000) 4038.

[13] P. I. Clemenson, A. E. Underhill, M. B. Hursthouse, R. L. Short, J. Chem. Soc., Dalton Trans. (1989) 61.

[14] A. Kobayashi, Y. Sasaki, Bull. Chem. Soc. Jpn. 50 (1977) 2650.

[15] J. C. Fitzmaurice, A. M. Z. Alexandra, D. J. Williams, J. D. Woollins, A. J. Lindsay, Polyhedron 9 (1990) 1561.

[16] Scott, J. C. *Highly Conducting Quasi-One-Dimensional Organic Crystals*; Semiconductors and Semimetals Series Vol. 27; Conwell, E., Ed.; Academic Press: New York, 1988, 385. (b) Kahn, O. *Molecular Magnetism*; VCH: New York, 1993.

[17] E. Coronado, M. Drillon, P. R. Nugteren, L. J. de Jongh, D. Beltran, J. Am. Chem. Soc. 110 (1988) 3907.

[18] J.W. Hall, W.E. Marsh, R.R. Weller, W.E. Hatfield, Inorg. Chem. 20 (1981) 1033.

[19] (a) C. Finazzo, M. Fontana, S. V. Doorslaer, W. Caseri, A. Schweiger, Phys. Chem. Chem. Phys. 7 (2005) 405; (b) R. Kirmse, W. Dietzsch, B. V. Solov'ev, J. Inorg. Nucl. Chem. 39 (1977) 1157.

[20] R. H. Holm, A. Davison, Inorg. Synth. 10 (1967) 8.

[21] T. Mori, A. Kobayashi, Y. Sasaki, H. Kobayashi, G. Saito, H. Inokuchi, Bull. Chem. Soc. Jpn. 57 (1984) 627.

[22] SAINT+: Area Detector Integration Software, Siemens Analytical Instruments Inc., Madison, WI (1995).

[23] G.M. Sheldrick, SADABS: Program for Semi-empirical Absorption Correction, University of Göttingen, Germany (1997).

[24] G.M. Sheldrick, Program for the Solution for Crystal Structures, University of Göttingen, Germany (1997).

[25] ORTEP-3 for Windows: L.J. Farrugia, J. Appl. Cryst. 30 (1997) 565.

Figure Legends

Fig. 1. Structural formula of tetra-*n*-butylammonium bis(maleonitriledithiolato)platinate(1–).

Fig. 2. (a) Packing diagram of the α-form viewed along the *b*-axis. (b) ORTEP [25] drawing of the molecular arrangement of the anions. Intermolecular contacts are shown as dashed lines, and the corresponding distances in the isomorphic nickel complex are shown in parentheses. Thermal ellipsoids are drawn at the 20% probability level, and hydrogen atoms are omitted for clarity.

Fig. 3. (a) Packing diagram of the β-form viewed along the *a*-axis. (b) ORTEP drawing of the molecular arrangement of the tetramer anion unit. Thermal ellipsoids are drawn at the 20% probability level, and hydrogen atoms are omitted for clarity.

Fig. 4. Temperature dependence of magnetic susceptibility for the α-form polycrystals, represented in the form $\chi_m T$ versus T.

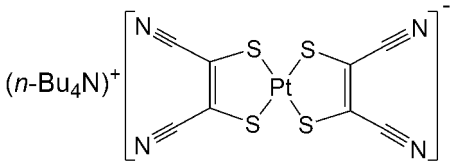

Fig. 1

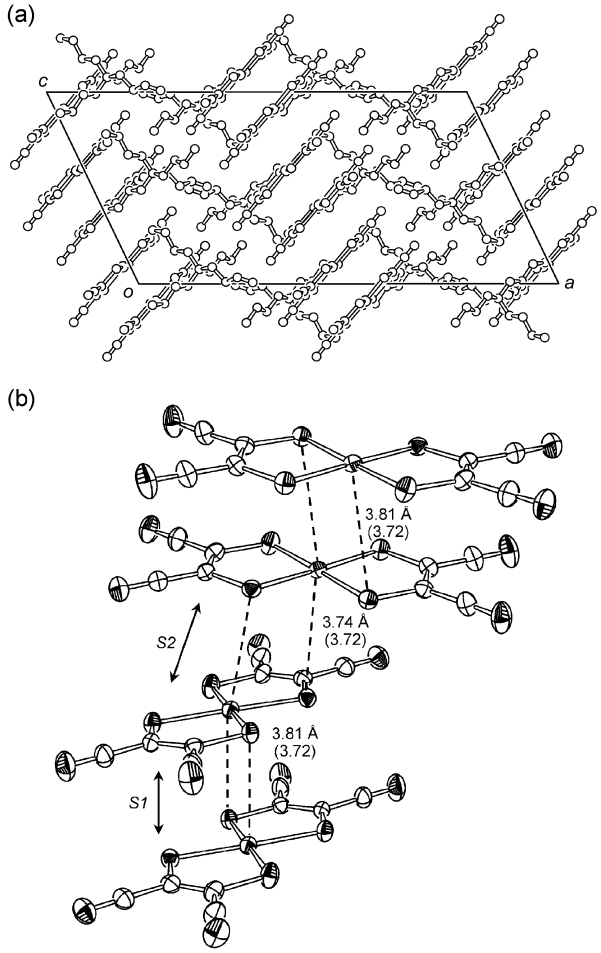

Fig. 2

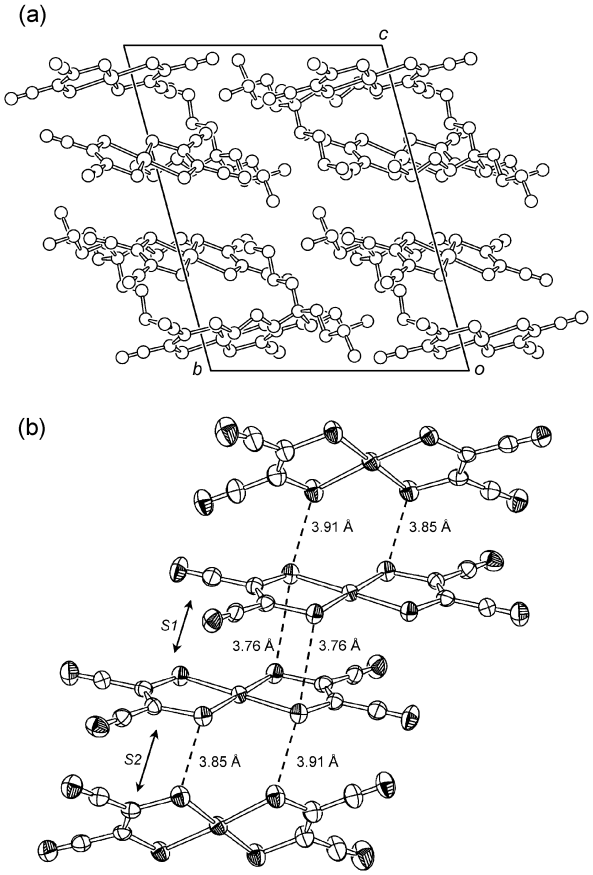

Fig. 3

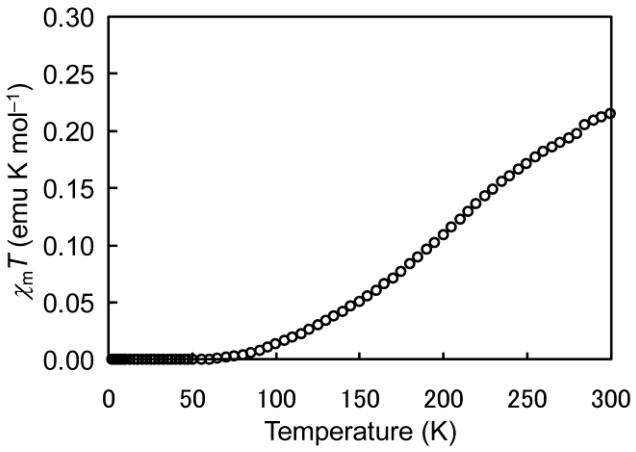

Fig. 4

Table 1		
Crystallographic data		
	α-form	β-form
Formula	$C_{24}H_{36}N_5PtS_4$	$C_{24}H_{36}N_5PtS_4$
Formula weight	717.91	717.91
T / K	298	298
Crystal system	Monoclinic	Triclinic
Space group	C 2/c	$P-1$
a / Å	30.847(2)	13.4636(9)
b / Å	13.8689(8)	13.6015(9)
c / Å	15.7393(9)	17.729(1)
α / °		73.379(2)
β / °	115.442(1)	78.933(2)
γ / °		78.181(1)
V / Å^3	6080.6(6)	3014.0(3)
Z	8	4
ρ_{calcd} / g cm^{-3}	1.568	1.582
μ(Mo-Kα) / cm^{-1}	49.11	49.35
Refl. / Parameter ratio	24.27	14.36
R_1, R_w[a]	0.0306; 0.0714	0.045; 0.102
Goodness of fit	1.03	1.02

[a] $R_1 = \Sigma||F_o| - |F_c|| / \Sigma|F_o|$; $R_w = [\Sigma w(F_o^2 - F_c^2)^2 / \Sigma w(F_o^2)^2]^{1/2}$